Paper ID: ET-04

Performance of Nanofluid with different Nanoparticles inside a solar collector

Rehena Nasrin*, Salma Parvin and M.A. Alim

Department of Mathematics, Bangladesh University of Engineering & Technology,
Dhaka-1000, Bangladesh.

**E-mail: rehena@math.buet.ac.bd*

Abstract

The forced convective flow and heat transfer characteristics of nanofluid inside a flat plate solar collector is analyzed numerically. The water- alumina/copper nanofluid and water-alumina nanofluid are used as the operational fluids through the fluid passing pipe of the solar collector. The governing partial differential equations with proper boundary conditions are solved by Finite Element Method using Galerkin's weighted residual scheme. The behaviors of nanofluids using both nanoparticles and single nanoparticle related to the performance such as temperature and velocity distributions, average heat transfer, collector efficiency, mean temperature and velocity are investigated systematically. These performances include the solid volume fraction namely ϕ of nanoparticles. The results show that the better performance of heat loss through the pipe of the flat plate solar collector is found by using the alumina and copper nanoparticles than only alumina nanoparticle.

Keywords: Forced convection, flat plate solar collector, finite element method, water based nanofluid with double nanoparticles.

1. Introduction

Of all the sources of renewable energy especially solar energy has the greatest potential when other sources in the country have depleted. Because of the desirable environmental and safety aspects it is widely believed that solar energy should be utilized instead of other alternative energy forms, even when the costs involved are slightly higher. Solar technologies are broadly characterized as either passive solar or active solar depending on the way they capture, convert and distribute solar energy. It will increase countries' energy security through reliance on an indigenous, inexhaustible and mostly import-independent resource, enhance sustainability, reduce pollution, lower the costs of mitigating climate change and keep fossil fuel prices lower than otherwise. These advantages are global. The fluids with solid-sized nanoparticles suspended in them are called "nanofluids". Applications of nanoparticles in thermal field are to enhance heat transfer from solar collectors to storage tanks, to improve efficiency of coolants in transformers.

There are so many methods introduced to increase the efficiency of the solar water heater by Xiaowu and Hua [1], Xuesheng et al. [2], Hussain [3] and Ho and Chen [4]. But the novel approach is to introduce the nanofluids in solar water heater instead of conventional heat transfer fluids (like water). The poor heat transfer properties of these conventional fluids compared to most solids are the primary obstacle to the high compactness and effectiveness of the system. The essential initiative is to seek the solid particles having thermal conductivity of several hundred times higher than those of conventional fluids. The suspended metallic or nonmetallic nanoparticles change the transport properties and heat transfer characteristics of the base fluid. Hwang et al. [5] studied the stability and thermal conductivity characteristics of nanofluids. In this study, they concluded that the thermal conductivity of ethylene glycol was increased by 30%.The absorptance of the collector surface for shortwave solar radiation depends on the nature and colour of the coating and on the incident angle. Usually black colour is used. Various colour coatings had been proposed in Tripanagnostopoulos et al. [6], Orel et al. [7] and Wazwaz et al. [8] mainly for aesthetic reasons. A low-cost mechanically manufactured selective solar absorber surface method had been proposed by Konttinen et al. [9]. The principal requirement of the solar collector is a large contact area between the absorbing surface and the air. Kent [10] studied laminar natural convection in isosceles triangular enclosures for cold base and hot inclined walls numerically. Nasrin et al. [11-12] analyzed effective heat transfer phenomena by different nanofluids on natural convection inside a solar collector.

From the literature review it is mentioned that no numerical or experimental work has been done introducing a nanofluid having different nanoparticles. In this paper, we investigate numerically the forced convection through the fluid passing pipe of a flat plate solar collector utilizing water based nanofluids having double nanoparticles such as alumina and copper as well as single nanoparticle alumina. So, the objective of this article is to present flow and heat transfer phenomena by a nanofluid with two nanoparticles through a solar collector.

2. Problem Formulation

Fig. 1 shows a schematic diagram of a solar collector. The fluid in the collector is water-based nanofluid containing Al_2O_3 and Cu nanoparticles. The nanofluid is assumed incompressible and the flow is considered to be laminar. It is considered that water and all nanoparticles are in thermal equilibrium and no slip occurs among them. It is assumed that both the nanoparticles are spherical shaped and diameters are 5 nm. The density of the nanofluid is approximated by the Boussinesq model. The governing equations for steady laminar forced convection flow in terms of the Navier-Stokes and energy equation (dimensional form) are given as:

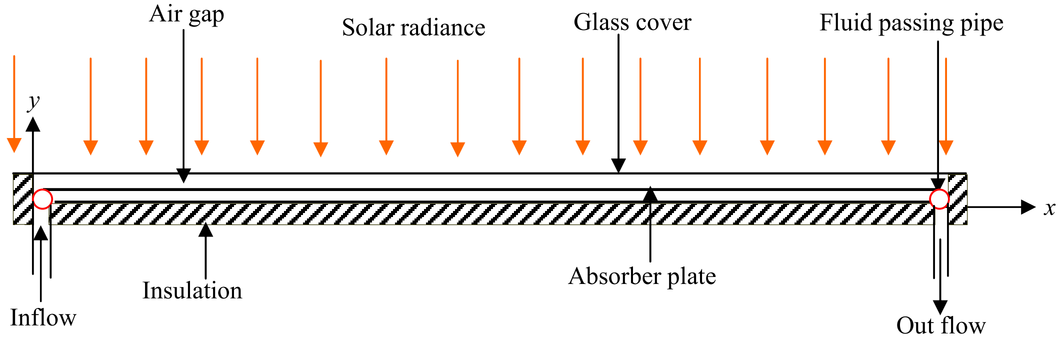

Fig. 1: Schematic diagram of the solar collector

The non-dimensional equations for forced convective flow are

$$\frac{\partial U}{\partial X}+\frac{\partial V}{\partial Y}=0 \tag{1}$$

$$U\frac{\partial U}{\partial X}+V\frac{\partial U}{\partial Y}=-\frac{\rho_f}{\rho_{nf}}\frac{\partial P}{\partial X}+\frac{1}{Re}\frac{\nu_{nf}}{\nu_f}\left(\frac{\partial^2 U}{\partial X^2}+\frac{\partial^2 U}{\partial Y^2}\right) \tag{2}$$

$$U\frac{\partial V}{\partial X}+V\frac{\partial V}{\partial Y}=-\frac{\rho_f}{\rho_{nf}}\frac{\partial P}{\partial Y}+\frac{1}{Re}\frac{\nu_{nf}}{\nu_f}\left(\frac{\partial^2 V}{\partial X^2}+\frac{\partial^2 V}{\partial Y^2}\right) \tag{3}$$

$$U\frac{\partial \theta}{\partial X}+V\frac{\partial \theta}{\partial Y}=\frac{1}{Re\,Pr}\frac{\alpha_{nf}}{\alpha_f}\left(\frac{\partial^2 \theta}{\partial X^2}+\frac{\partial^2 \theta}{\partial Y^2}\right) \tag{4}$$

where $Pr=\frac{\nu_f}{\alpha_f}$ is Prandtl number, $Re=\frac{U_i L}{\nu_f}$ is Reynolds number, $\rho_{nf}=(1-\phi_1-\phi_2)\rho_f+\phi_1\rho_{s1}+\phi_2\rho_{s2}$ is density, $(\rho C_p)_{nf}=(1-\phi_1-\phi_2)(\rho C_p)_f+\phi_1(\rho C_p)_{s1}+\phi_2(\rho C_p)_{s2}$ is heat capacitance, $\alpha_{nf}=k_{nf}/(\rho C_p)_{nf}$ is the thermal diffusivity, the effective viscosity of the nanofluid by the Pak and Cho correlation [13] is taken as modified form $\mu_{nf}=\mu_f\left\{1+39.11(\phi_1+\phi_2)+533.9(\phi_1^2+\phi_2^2)\right\}$ and the effective thermal conductivity (modified form) of Maxwell Garnett (MG) model [14] is $k_{nf}=k_f\frac{(k_{s1}+k_{s2})+2k_f-2\phi_1(k_f-k_{s1})-2\phi_2(k_f-k_{s2})}{(k_{s1}+k_{s2})+2k_f+\phi_1(k_f-k_{s1})+\phi_2(k_f-k_{s2})}$.

The above equations are obtained by using the following dimensionless dependent and independent variables

$$X=\frac{x}{L},\ Y=\frac{y}{L},\ U=\frac{u}{U_i},\ V=\frac{v}{U_i},\ P=\frac{p}{\rho_f U_i^2},\ \theta=\frac{T-T_i}{T_c-T_i}$$

If I is the intensity of solar radiation, in W/m^2, incident on the aperture plane of the solar collector having a collector surface area of A, m^2, then the amount of solar radiation received by the collector is: $Q_i=I.A$

Basically, it is the product of the rate of transmission of the cover (λ) and the absorption rate of the absorber (κ). Thus, $Q_i=I(\lambda\kappa)A$

The rate of heat loss (Q_o) depends on the collector overall heat transfer coefficient (h) and the collector temperature $Q_o=hA(T_c-T_a)$.Thus, the rate of useful energy extracted by the collector (Q_u), expressed as a rate of extraction under steady state conditions, is proportional to the rate of useful energy absorbed by the collector, less the amount lost by the collector to its surroundings. This is expressed as:

$Q_u = Q_i - Q_o = I(\lambda\kappa)A - hA(T_c - T_a)$, where T_c and T_a are the temperature of the collector and ambient temperature outside the collector. The rate of extraction of heat from the collector may be measured by means of the amount of heat carried away in the fluid passed through it, that is: $Q_u = mC_p(T_o - T_i)$

A measure of a flat plate collector performance is the collector efficiency (η) defined as the ratio of the useful energy gain (Q_u) to the incident solar energy over a particular time period:

$$\eta = \frac{\text{useful gain}}{\text{available energy}} = \frac{mC_p(T_o - T_i)}{AI}$$

where m is the mass flow rate of the fluid flowing through the collector; C_p is the specific heat; and T_i and T_o are the mean fluid inlet and outlet temperatures, respectively. The computation domain is the fluid passing pipe which is attached to the absorber plate. At the top and bottom walls of the pipe maintain heat flux $q = I(\lambda\kappa)A - hA(T_c - T_a)$.

The dimensionless boundary conditions are:

at the top and bottom walls of the pipe: non-dimensional heat flux

at the inlet opening: $\theta = 0$, $U = 1$

at all solid boundaries of the pipe: $U = V = 0$

at the outlet opening: convective boundary condition $P = 0$

The average Nusselt number at the top surface of the pipe takes the form $Nu = -\int_0^1 \left(\frac{k_{nf}}{k_f}\right)\frac{\partial\theta}{\partial Y}dX$. The mean bulk temperature and average velocity of the fluid may be written as $\theta_{av} = \int \theta \, d\bar{V} / \bar{V}$ and $V_{av} = \int V \, d\bar{V} / \bar{V}$, where $\bar{V}$ is the volume of the pipe.

3. Numerical Approach

The Galerkin finite element method of Taylor and Hood [15] and Dechaumphai [16] is used to solve the considered problem. The equation of continuity has been used as a constraint due to mass conservation and this restriction may be used to find the pressure distribution. The finite element method is used to solve the Eqs. (2) - (4), where the pressure P is eliminated by a constraint. The continuity equation is automatically fulfilled for large values of this constraint. Then the velocity components and temperature are expanded using a basis set. The Galerkin finite element technique yields the subsequent nonlinear residual equations. Three points Gaussian quadrature is used to evaluate the integrals in these equations. The non-linear residual equations are solved using Newton–Raphson method to determine the coefficients of the expansions. The convergence of solutions is assumed when the relative error for each variable between consecutive iterations is recorded the convergence criterion ε. The thermophysical properties of the nanofluid are taken from Ogut [17] and given in Table 1.

Table 1: Thermo-physical properties of base fluid and different nanoparticles

Physical Properties	Fluid phase (Water)	Al_2O_3	Cu
C_p(J/kgK)	4179	765	385
ρ (kg/m^3)	997.1	3970	8933
k (W/mK)	0.613	40	400
$\alpha \times 10^7$ (m^2/s)	1.47	131.7	1163.1

3.1 Grid Independent Test

An extensive mesh testing procedure is conducted to guarantee a grid-independent solution for Re = 400 and Pr = 6.6 in a solar collector. In the present work, five different non-uniform grid systems with the following number of elements within the resolution field are examines: 60, 240, 960, 3840 and 15360. The numerical scheme is carried out for highly precise key in Nu for water-Al_2O_3 nanofluid (ϕ = 5%) as well as base fluid (ϕ = 0%) for the aforesaid elements to develop an understanding of the grid fineness as shown in Table 2. The scale of the average Nusselt numbers for 3840 elements shows a little difference with the results obtained for the other elements. Hence, considering the non-uniform grid system of 3840 elements is preferred.

Table 2: Grid Sensitivity Check at Pr = 6.6, ϕ = 5% (water/alumina nanofluid) and Re = 400

Nodes (elements)	506 (60)	1788 (240)	6692 (960)	25860 (3840)	101636 (15360)
Nu (nanofluid)	7.82945	9.19176	10.17518	10.84991	10.85001
Nu (basefluid)	6.62945	7.99976	8.88701	9.551698	9.551718
Time (s)	126.265	312.594	398.157	481.328	929.377

3.2 Code Validation

The present numerical solution is validated by comparing the current code results for collector efficiency - temperature difference [T_i - T_a] profile of water with the graphical representation of Kalagorirou [18] for flat plate solar thermal collector at irradiation level 1000 W/m^2. Solar thermal collectors and applications were reported by Kalagorirou [18]. Fig. 2 demonstrates the above stated comparison.

4. Results and Discussion

In this section, numerical results of isotherms and streamlines for various values of solid volume fraction ($\phi = \phi_1 + \phi_2$) of Al_2O_3/Cu /water nanofluid through a fluid passing pipe of a flat plate solar collector are displayed. The considered values of ϕ are ϕ (= 1%, 3%, 5%, 7% and 10%) while the Prandtl number Pr = 6.6 and Re = 400 are kept fixed.

The effect of ϕ (= $\phi_1 + \phi_2$) on the thermal, velocity and heat flux fields are presented in Fig. 3 (a)-(c). Increasing ϕ (solid volume fraction of alumina and copper nanoparticles equally), the temperature lines near the upper and lower parts of the riser pipe become flatten whereas at the lower ϕ (= 1% = 0.5% + 0.5%) they are bended due to concentration of solid particles is dominated across the pipe. With the rising values of ϕ from 1% to 5%, the temperature distributions become distorted resulting in an increase in the overall heat transfer. This is because the thermal conductivity of the solid particles is very high. This means that higher heat transfer rate is predicted by the nanofluid having two nanoparticles namely Al_2O_3 and Cu. It is worth noting that as the solid volume fraction of Al_2O_3 and Cu nanoparticles increases, the thermal boundary layer near the top and bottom surfaces of the riser pipe becomes thick which indicates a steep temperature gradients and hence, an increase in the overall heat transfer from the absorber plate containing pipe to the outlet edge. But further increasing ϕ to 10% (= 5% + 5%) there is no perturbation observed in the isothermal lines at all. Thus adding more solid volume fraction is not advantageous.

The corresponding velocity field indicates that at ϕ = 1% the velocity of nanofluid is high. Thus the nanofluid quickly passes the pipe by getting heat from upper and lower walls as a result the streamlines appear the whole riser pipe. In the velocity vector, initially the flow covers the entire domain of the pipe while it concentrates near the middle of the pipe of flat plate solar collector due to increase solid volume fraction ϕ from 1% (= 0.05% + 0.05%) to 10% (= 5% + 5%) of water-alumina/copper nanofluid. This happens because of escalating solid concentrations of flow. Nanofluid having larger density does not move freely.

The heatlines are smooth and it is observed that the lines are perfectly perpendicular to the isothermal lines and the upper and lower walls. This further indicates that the heat flow is conduction dominant. From the Fig. 5(c) it is clearly observed that the heatlines with greater strength become smaller in size at the middle of the flow pipe for ϕ = 5% (2.5%+2.5%). This happens due to more thermal conductive heat flux and as it is seen the case of the lowest solid volume fraction, the strength of heatline goes to low. The heatlines remain constant for further increasing ϕ from 5% to 10%. This means that major amount of heat flux or transport occurs for ϕ = 5% of water-Al_2O_3/Cu nanofluid.

In Fig. 4(i)-(iii) average Nusselt number (Nu) at the upper hot surface, mean temperature (θ_{av}), magnitude of average velocity vector (V_{av}) with various solid volume fraction is accounted for nanofluid having double and single nanoparticle as well as clear water. Nu enhances sharply with growing ϕ upto 5% and then remains unchanged with advance mixture of solid volume faction for water based nanofluid having double as well as single nanoparticles. Rate of heat transfer enhances by 15% and 11% with the variation of ϕ from 1% to 5% for water-alumina/copper and water-alumina nanofluids respectively. Fig. 4(ii) displays that θ_{av} grows sequentially for ϕ upto 5% for both mixture of nanofluid. Mean temperature remains constant for further increasing values of solid volume fraction from 5% to 10%. It is well known that total thermal conductivity of Al_2O_3 and Cu nanoparticles is higher than only Al_2O_3 nanoparticle. Higher thermal conductivity is capable to carry more heat. Thus average bulk temperature of water-Al_2O_3/Cu nanofluid has found higher. There is no change of water (ϕ = 0%) due to the deviation of nanoparticles volume fraction. Consequently V_{av} has notable changes with different values of solid concentration of different mixtures of nanofluid. Growing ϕ devalues mean velocity of the nanofluid through the riser pipe of the flat plate solar collector. Here water-alumina nanofluid has higher mean velocity than the water-alumina/copper nanofluid. Less solid concentrated nanofluid has greater velocity than highly concentrated nanofluid.

Fig. 5(i)-(ii) expresses the collector efficiency η (%)-solid volume fraction ϕ (%) for the nanofluid with single and double nanoparticles and mid-height temperature (dimensional) of water-alumina/copper nanofluid. From Fig. 5(i) it is observed that adding low quantities of nanoparticles leads to the remarkable enhancement of the efficiency until a volume fraction of approximately 5%. After a volume fraction of 5%, the efficiency begins to level off with increasing volume fraction. The authors attribute this unchanging to the high increase of the fluid absorption at high particle loadings. The main difference in the steady-state efficiency occurs in water based nanofluid having alumina and copper nanoparticles. Collector efficiency rises from 44% to 58% and from 44%

to 54% with growing the solid volume fraction ϕ from 0% to 5% for water based nanofluid having double and single nanoparticles respectively. On the other hand the inlet temperature of fluid is maintained at 300K and then it increases gradually with the contact of heated upper and lower solid boundaries of the riser pipe. And finally the output temperature of water-alumina/copper nanofluid becomes 344K, 350K, 354K, 358K, 358K and 358K for $\phi = 0\%$, 1%, 3%, 5%, 7% and 10% respectively.

5. Conclusion

The results of the numerical analysis lead to the following conclusions:

- The structure of the fluid isotherms and streamlines through the pipe is found to significantly depend upon the solid volume fraction of water-alumina/copper nanofluid.
- The Al_2O_3/Cu nanoparticles with $\phi = 5\%$ are established to be more effective in enhancing performance of heat transfer rate than Al_2O_3 nanoparticle.
- Collector efficiency rises for nanofluid having two nanoparticles than nanofluid with single nanoparticle.
- Mean temperature rises for water- Al_2O_3/Cu nanofluid than water- Al_2O_3 nanofluid.
- Average velocity field devalues due to growing ϕ.

6. References

[1] W. Xiaowu, B. Hua, "Energy analysis of domestic-scale solar water heaters", *Renew. Sustain Energy Rev.*, Vol. 9, No. 6, pp. 638–645, 2005.

[2] W. Xuesheng, W. Ruzhu, W. Jingyi, "Experimental investigation of a new-style double-tube heat exchanger for heating crude oil using solar hot water", *Appl. Therm. Eng.*, Vol. 25, No. 11-12, pp. 1753–1763, 2005.

[3] A. Hussain, "The performance of a cylindrical solar water heater", *Renew. Energy*, Vol. 31, No. 11, pp. 1751–1763, 2006.

[4] CD. Ho, TC. Chen, "The recycle effect on the collector efficiency improvement of double-pass sheet-and-tube solar water heaters with external recycle", *Renew. Energy*, Vol. 31, No. 7, pp. 953–97, 2006.

[5] Y. Hwang, JK. Lee, CH. Lee, YM. Jung, SI. Cheong, CG. Lee, BC. Ku, SP. Jang, "Stability and thermal conductivity characteristics of nanofluids", *Thermochimica Acta*, Vol. 455, No. 1–2, pp. 70–74, 2007.

[6] Y. Tripanagnostopoulos, M. Souliotis, Th. Nousia, "Solar collectors with colored absorbers", *Solar Energy*, Vol. 68, pp. 343–356, 2000.

[7] ZC. Orel, MK. Gunde, MG. Hutchins, "Spectrally selective solar absorbers in different non-black colours", *Proceedings of WREC VII*, Cologne on CD-ROM, 2002.

[8] J. Wazwaz, H. Salmi, R. Hallak, "Solar thermal performance of a nickel-pigmented aluminium oxide selective absorber", *Renew. Energy*, Vol. 27, pp. 277–292, 2002.

[9] P. Konttinen, PD. Lund, RJ. Kilpi, "Mechanically manufactured selective solar absorber surfaces", *Solar Energy Mater. Solar Cells*, Vol. 79, No. 3, pp. 273–283, 2003.

[10] E.F. Kent, "Numerical analysis of laminar natural convection in isosceles triangular enclosures for cold base and hot inclined walls", *Mechanics Research Commun.*, Vol. 36, pp. 497–508, 2009.

[11] R. Nasrin, MA. Alim, and AJ. Chamkha, "Effects of physical parameters on natural convection in a solar collector filled with nanofluid", *Heat Transfer-Asian Research*, Vol. 42, No. 1, pp. 73-88, 2013.

[12] R. Nasrin, MA. Alim, and AJ. Chamkha, "Modeling of double diffusive buoyant flow in a solar collector with water-CuO nanofluid", *Heat Transfer-Asian Research*, Vol. 42, No. 3, pp. 212-229, 2013.

[13] BC. Pak, Y. Cho, "Hydrodynamic and heat transfer study of dispersed fluids with submicron metallic oxide particle", *Experim. Heat Transfer*, Vol. 11, pp. 151-170, 1998.

[14] JC. Maxwell-Garnett, "Colours in metal glasses and in metallic films", *Philos. Trans. Roy. Soc. A* Vol. 203, pp. 385–420, 1904.

[15] C. Taylor, P. Hood, "A numerical solution of the Navier-Stokes equations using finite element technique", *Computer and Fluids*, Vol. 1, pp. 73–89, 1973.

[16] P. Dechaumphai, "Finite Element Method in Engineering", 2nd ed., Chulalongkorn University Press, Bangkok, 1999.

[17] EB. Ogut, "Natural convection of water-based nanofluids in an inclined enclosure with a heat source", *Int. J. of Thermal Sciences*, 48, 1–11, 2009.

[18] S.A. Kalogirou, Solar thermal collectors and applications, *Progress in Energy and Combustion Science*, 30, 231–295, 2004.

$X = \frac{x}{L}, Y = \frac{y}{L},$

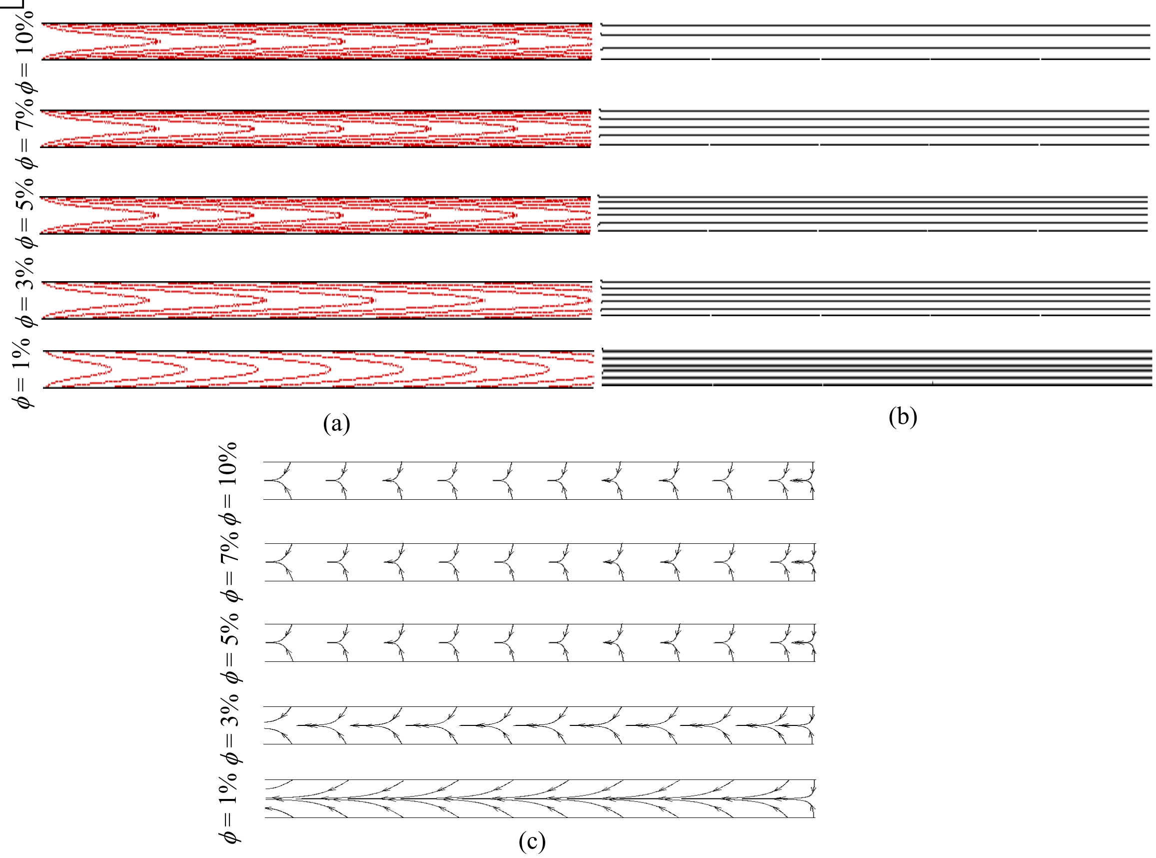

Fig. 3: Effect of ϕ of water-alumina/copper nanofluid on (a) temperature, (b) streamfunction and (c) heatfunction

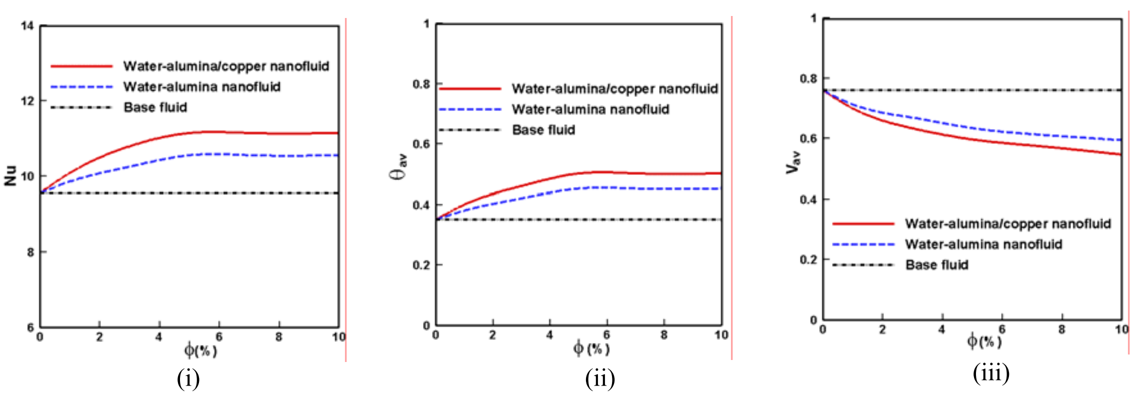

Fig. 4: Effect of ϕ of nanofluid with single and double nanoparticles on (i) Nu, (ii) θ_{av} and (iii) V_{av}

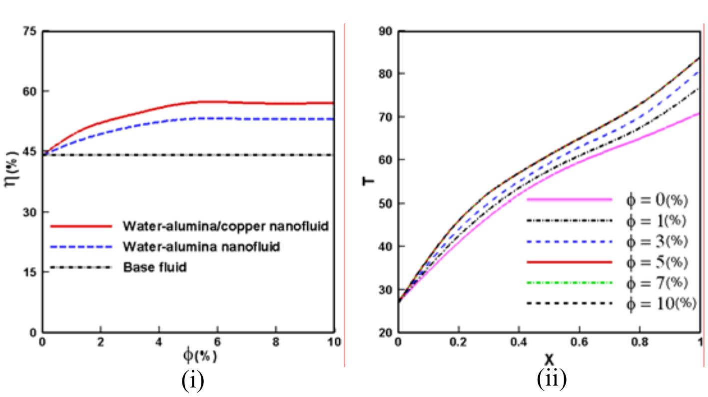

Fig. 5: Plots of (i) η and (ii) mid-height temperature

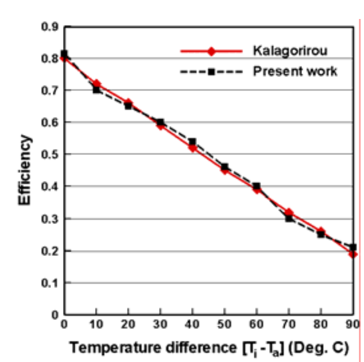

Fig. 2: Comparison of present code with Kalagorirou [18] at $I = 1000$ W/m^2